Session 4 - Hot Film Measurements

BOUNDARY LAYER TRANSITION DETECTION ON SUCTION SIDES OF HIGH-DEFLECTION TURBINE BLADE CASCADES

F. Pittaluga & G. Benvenuto

Dept. of Energy Engineering
The University of Genova, Italy

SUMMARY

At the Energy Engineering Department of Genova University two adaptive wall transonic cascade tunnels have recently become fully operative, one aimed at probe calibration and low deflection blade cascade testing, the other one at high deflection cascades. The test section of the latter, with an Ansaldo root section cascade installed, has been reconfigured in order to allow the following measurements to be taken even simultaneously:

- closed circuit tv-overview of the overall flow processes taking place in each of the 15 blade channels of the cascade during flexible walls adjustments
- test section side walls static pressure measurements
- aerodynamic probe traverses upstream and downstream of blades
- pressure behavior on the contour of a whole blade channel
- schlieren visualization through optical glass windows
- transition detection on blades' suction sides

The experimental technique specifically set up for detecting boundary layer transition relies on multi-sensor (8 filaments) hot-film surface probes of the glue-on type, mounted flush on the blade suction surface in order to induce no intrusive effects onto the boundary layers, though thin and laminar. Transition from laminar to turbulent boundary layer flow is traced through rms analysis of the fluctuating signals coming from the probe.

The paper discusses the technological aspects of the method, the instrumentation characteristics and the probe responses with the aim of correlating them to the boundary layer regimes. Preliminary blade transition region localizations are given. Future developments are needed and are already under way, even toward re-laminarization region detection expected to take place shortly upstream of blades' trailing edges.

1. INTRODUCTION

In recent years the main objective of transonic experimentation carried out at DINE, the Energy Engineering Department of Genova University, has been that of achieving a most clear picture, compatible with the intrinsic difficulties of the problem, of the complex fluid-dynamics phenomena governing performance, in particular viscous losses, of turbine blade cascades operating in the transonic range. From the beginning, avoiding unaffordable provision of large transonic facilities, the design choice for the cascade tunnels to be installed was that of providing, wherever possible, continuous adaptivity to test section upper and lower walls, in order to gain effective control of flow behaviour toward periodicity improvement, wall interference relief, transonic blockage and shock reflections minimization (ref. [1,2,3,4,5]).

To this aim, the transonic facilities installed and now operative at DINE are synthetically as follows:

TUNNEL TRS-1 :
- Adaptive Wall Facility for Probe Calibration
- 36 jacks lower wall; 36 jacks upper wall
- Test Section (rectangular) : 200 x 50 mm
- Mach Number Range : up to 2.0
- Operation : suction, continuous

TUNNEL TRP-1 :
- Adaptive Wall Facility for Cascade Testing
- Cascade Deflection : up to 40 deg
- Tunnel characteristics : same as above, since TRS-1 can be easily converted to TRP-1 by replacement of its test section

TUNNEL TRP-2 :
- Adaptive Wall Facility for Cascade Testing
- Cascade Deflection : from 40 to 150 deg
- Nozzle and test section angularly and independently orientable
- Test section bottom wall and diffuser walls : flexible, fully adaptive, 13 + 26 jacks
- Cascade length : up to 300 mm
- Test section depth : 50 mm
- Mach number range : up to 2.0
- Operation : suction, continuous

The test sections of the above tunnels are presented in figures 1,2 and 3 respectively.

Aim of this paper is to discuss the latest developments and experimental outcome achieved with a root-section turbine blade cascade installed in tunnel TRP-2, specifically instrumented toward the simultaneous detection of both the overall flow behavior and some critical parameters governing the boundary layer flows, such as surface heat transfer and transition to turbulence.

Actually, as is well documented in literature, the problem of predicting the boundary layer regimes along turbine blade surfaces, in particular the onset to turbulent conditions, is becoming vital in order to assess blade performance, in terms of surface heat transfer and loss coefficients (ref. [6, 7,8,9]). With particular reference to hub sections of last stage rotor blades for large steam turbines, characterized by high loss levels due to the long passages with little or no contraction (ref. [10]), almost nothing is known about boundary layers' conditions. An instrumented blade of this latter type has been the object of the experimental research here reported, carried out using, in addition to standard transonic cascade instrumentation, also a novel multi-sensor hot film probe mounted flush on the suction surface of a blade, in order to detect the behavior of the time-dependent surface heat transfer in the transitional region and to correlate it to the fluid-dynamic boundary layer conditions.

2. THE EXPERIMENTAL SET-UP

The cascade tunnel TRP-2, whose design and operational characteristics are described in ref. [6], has been provided with a reconfigured test section, equipped with two optical glass (90 x 90 mm) removable windows for high-quality flow visualizations. Upstream and downstream of the cascade two computer-controlled (no-backlash) probe traversing gears are outfitted: the miniaturized aerodynamic probes, typically either of the combined "needle" type or of the AVA "wedge" type, are manufactured through innovative techniques like photo-chemical machining and electron-discharge process (ref.[2]).

The cascade mounted in the tunnel is made up of 16 blades with a root-section profile designed by Ansaldo in 1985; its main features are the following:

- Identification: PRG 529 - root 26"/72"
- Axial chord: 60.17 mm
- Tangential pitch: 17.60 mm
- Throat: 9.171 mm
- Throat/pitch: 0.521
- Design inlet angle: 32.2 deg
- Design deflection: 114.5 deg
- "Nominal" inlet Mach number: 0.80
- "Nominal" outlet Mach number: 0.90

The cascade was manufactured through electron discharge "wire" machining, whilst the holes for the blades' pins were worked into the test section side walls by means of computer controlled machining in order to preserve periodical geometry. The test section with the cascade installed, the traversing gears and the schlieren optical apparatus with the closed-circuit television set are shown in figs. 4 and 5.

The cascade mid-channel is instrumented with 24 + 25 static tappings, respectively on the pressure and suction blade surfaces, connected (as is also the case for the aerodynamic probes on the gears, and the taps on the side walls) to both multimanometer readings and to a series of pressure transducers (Schaewitz transducers of different measuring range) for data acquisition. To this end a Hewlett-Packard 9816 computer is utilized, which also supervises and backups the traverse electronic controller.

3. THE TRANSITION DETECTION INSTRUMENTATION

As above said, the main reason of the research was that of gaining some insight into the boundary layer conditions along the suction surface of a blade whose design is strongly affected by mechanical requirements, such as the large cross sectional area of the profile and the small pitch, so that the loss level is high, usually of the order of 10% or more.

In the case here discussed, losses turned out higher than expected due to flow separations taking place near outlet, brought about by too thin trailing edges, inducing excessive rear suction side curvatures. Detailed experimental results and blade performance analysis are given in ref. [6], from which the Mach number distributions along the blade surfaces and the loss coefficient behavior are taken and here presented in figs. 6 and 7.

In order to localize boundary layer instability point and transition zone, attention was focused right after the suction side velocity peak taking place (fig. 6) around x = 7% chord, which is more or less common to all blades of this kind (ref. [10]). In order to induce no intrusive effects onto the boundary layer, expectedly very thin and laminar at least up to that location, a probe had to be selected which would not perturb the near surface flow parameters: choice was addressed toward recent types of multi-sensor hot film probes, produced by Dantec Elektronik (Denmark) upon customer design, to be mounted flush on the blade surfaces, to which tight adherence is assured by a sort of glue. Probe basic material is a thin (0.05 mm) sheet of 20.0 x 28.5 mm polyimide (Kapton) foil, upon which 8 sensing elements 0.2 x 1.0 mm, with respective leads, are directly deposited: the sensors are made in nickel, whilst the leads are in gold. To achieve perfect flush mounting, the blade surface was remachined, again with electron discharge process, in order to

recover exactly the blade geometry also where the probe was to be placed. The overall probe configuration, of which 4 prototypes have been ordered and manufactured, is shown in fig. 8: taking care of the location of the above discussed suction side velocity peak, the probe and its sensors were positioned as can be seen in fig. 9, i.e. with the probe' s forward rim localized at a distance s = 8.0 mm from the blade leading edge, so that the first sensor is found at s = 8.9 mm. Fig. 10 shows a blade instrumented with the probe, whilst in fig. 11 the blade is placed in cascade and mounted in the tunnel test section.

This type of thin film gauges, due to their extremely miniaturized dimensions, can yield a wide effective bandwith in surface heat transfer fluctuations detection, up to about 35 kHz, provided, as in the present case, that the electrical analogue circuits are coupled with high speed digital sampling instrumentation. This latter function was here performed by using a HP-5450-2A Digitizing Oscilloscope with 400 MHz bandwith, a sample rate of 400 MSamples/s, 2 channels, designed for both repetitive and single-shot signals; the time base range is from 1 ns/div to 5 s/div whilst the vertical sensitivity is from 2 mV/div to 5 V/div. The instrument features ample digital storage, real time measurement statistics and instant hardcopy over a graphics printer. The oscilloscope is pictured in fig. 12, together with a large part of the overall electronic instrumentation being used, such as the four DISA 55M10 Main Units, the traverse controller and the HP computer.

4. EXPERIMENTAL RESULTS

The detailed experimental and theoretical analysis previously carried out at nominal inlet incidence angle (zero) on the same blade here discussed, whose results are presented in ref. [6], has made it possible to proceed, as a logical extension of that research, toward a direct detection of the fluctuations which take place in the blade boundary layers downstream of the so called instability point, that is in the transitional region. In effect, the main objective of the investigation was that of trying to localize the onset and the extension of transition in the suction side boundary layers of a blade type which, to authors' knowledge, had never been studied experimentally from this point of view, leaving almost totally unanswered the questions regarding not only the respective extensions of the laminar, transitional and turbulent regimes, but also the presence of possible intra-blade boundary layer detachments. Furthermore, as far as the rather common presence, for these blades, of flow separations near outlet is concerned, it was considered important to find out if they should be traced to re-laminarization phenomena taking place in the turbulent boundary layers undergoing the strong accelerations induced by the last portion of the rear suction sides.

The concepts upon which the thin film technique is based are well documented (e.g. ref. [7,9]): in the present case the 8 sensors of a probe were heated, by a constant temperature bridge anemometer, above the recovery temperature of the flow, in order to measure the fluctuating heat transfer rates $\dot{q}$ between the sensors and the boundary layer flow. In reality, what is being measured is:

$$\dot{Q}_{tot} = \dot{q} + \dot{Q} + \dot{Q}_s$$

where $\dot{Q}$ is the mean heat transfer to the flow and $\dot{Q}_s$ is the heat transfer to the probe substrate sticked on the blade. Unfortunately, $\dot{Q}$ and $\dot{Q}_s$ cannot be

measured separately, so that the mean part of the heat transfer reading cannot be utilized toward detection, for example, of separation bubbles, where $\dot{Q}$ is expected to fall (but not $\dot{Q}_m$, which can assume misguiding behavior).

For this reason, at least so far, emphasis was placed mainly on the a.c. signals coming from the anemometers: in real time, during the tests, they were undergoing display on the oscilloscope screen, digitization, statistical analysis, push-button hard copy output. In order to compensate the small differences among sensors, the overheat ratios where slightly adjusted so to yield, in all cases, the same anemometer output mean level E: in this way, the fluctuating "e" voltages and their effective levels e_{rms}, assumed as representative of the fluctuating heat transfer rates $\dot{q}$, turned out, to some extent, normalized.

A typical no-flow trace of the anemometer a.c. output (e.g. that of sensor 1) is displayed in fig. 13: the vertical sensitivity of the oscilloscope is set to the near-maximum value of 4 mV/div and what is being detected is mainly electro-magnetic noise. At this point the tunnel is set into operation, at a $M_{2is} = 0.96$ downstream of cascade: the sensor 1 trace changes, assuming behavior shown in fig. 14, typical of a fully laminar situation (notice the setting of sensitivity to 40 mV/div), as confirmed by an effective value $e_{rms} = 1.673$ mV. The tunnel turbulence level at cascade inlet is low, of the order 1.2 percent and the blade surface roughness, as produced by the electron discharge machining, is very low, so that the process of transition will not be "forced" by these parameters.

With both the time-scale and the sensitivity settings held constant, for all readings, respectively at 500 μs/div and at 40 mV/div, all the sensor traces are organized together in fig. 15, with the exception of sensor n. 2, damaged before its use. It can be seen, as a preliminary outcome, that the probe was correctly positioned on the blade surface, since its sensors turn out localized exactly where transition process is starting and developing. A second remark is that no neat "transition point" exists, but, on the contrary, the "transition region" is extremely spread out.

To be precise, sensor 1 position is at 8.9 mm from leading edge (see figs. 8,9), which is 1.7 mm downstream of the velocity peak shown in fig. 6. The re-compression which takes place after this peak is very likely to be referred to a localized shock wave rather weak, possibly oscillating, since it does not show up in the schlieren visualization (fig. 16), taken with a continuous light source. What is most important, the said re-compression appears to be followed by a wide region of near-constant Mach number, as can be seen both in the same fig. 6 and in fig. 17, obtained through a theoretical analysis performed by means of a time marching technique already discussed in ref. [6].

If, at this time, we introduce (see fig. 18) the behavior of the effective values e_{rms} as evaluated upon the instantaneous fluctuating values e of fig. 15, the whole picture is ready for drawing some conclusions.

Boundary layer flow is fully laminar up to sensor 1 ($x/c \approx 0.08$ in fig. 6); then it interacts with the recompression induced by a localized shock wave. This interaction is pulsating, may even bring about a limited detachment, and is responsible for the lower-frequency fluctuations ($f \approx 1.8$ kHz) which show up in sensor 3 trace: these superposed oscillations are causing the "organized" turbulence-free increase in e_{rms} from sensor 1 to sensor 3 (fig. 18), however do not possess sufficient energy to overcome the damping capacity of the laminar boundary layer, whose trace, though fluctuating, appears of the same basic type for both sensors.

Something changes in sensor 4 trace ($s = 13.2$ mm; $x/c \approx 0.12$): low frequency oscillations are damped out whilst very small turbulent "spikes"

begin to appear. If one adds up all the instants of time interested by these turbulent bursts and normalizes the sum with respect to the total elapsed time, he can evaluate, at least roughly, the flow intermittency factor γ which turns out about 0.15. The behavior of e_{rms} for sensor 4 falls somewhat lower with reference to sensor 3 (fig. 18), due to the disappearance of the low frequency fluctuations, not yet balanced by the onset of the too small turbulent spots, and possibly due also to the mild acceleration which appears to take place just after the shock wave. Since γ is already different from zero at station 4, it can be inferred that the point of instability of the boundary layer is approximately localized around station 3.

Sensor 5 trace (s = 15.2 mm; x/c ≈ 0.14) shows a typical transitional behavior, where γ is around 0.5 and where the turbulence-like fluctuations still are characterized by a low amplification ratio and following a kind of a near-regular pattern in amplitude and frequency. This latter is in the order of 6 kHz and turns out uncorrelated to the Tollmien-Schlichting waves' frequency, which is two orders of magnitude higher in this case. This result can be interpreted in the light of the above discussed interaction with the shock wave that the boundary layer has undergone: this interaction has most likely destroyed the natural growth of the T.S. disturbances from the laminar into the transitional zone, giving rise, instead, to a "forced" instability and a transition inception with amplification of waves "tuned" on frequencies which are multiple of those of the above seen shock vibration.

Sensor 6 trace (s = 17.8 mm; x/c ≈ 0.166) shows random amplification of some fluctuations' amplitudes, whilst frequencies do not show a dominant one: a very rough estimate of γ is around 0.85. Residual laminar damping effects have so far "constrained" the amplitudes of the isolated turbulent spots: the situation can be named "transitional-laminar". From now on the spots start to merge ("transitional-turbulent" flow), with a strong increment in the fluctuations' amplitudes through stations 7 and 8.

Unfortunately, no sensor is available downstream of station 8, where the e_{rms} is still increasing, thus indicating that a fully turbulent condition has not yet been reached: however, it can be seen in fig. 18 that the trend of e_{rms} is almost topping at station 8 so that the end of transition is likely to take place shortly after. Since sensor 8 is positioned at s = 24.2 mm from leading edge, the very interesting result is achieved that, for the blade under investigation, transitional flow takes place, downstream of instability point, for at least 23% of suction surface length, and possibly more.

5. CONCLUSIONS

The experimental study here discussed, though preliminary under various aspects, has anyway already afforded to reach some conclusive outcome. First of all, the technological aspects of the non-intrusive mounting of the miniaturized hot-film probes in a transonic cascade test section have been fully mastered. The signal processing strategy is not yet completed, and soon will be supported by proper instrumentation performing spectral analysis: however, the use of an advanced multiple-function digitizing oscilloscope has turned out extremely suitable and effective.

The state of the boundary layer on a hub-section blade profile has been, probably for the first time, traced through the transitional process: the damping capacities of the laminar regime have been shown to succeed in preserving, to some extent unexpectedly, laminar character to the flow even during interaction with a shock wave. The same damping properties are respons-

ible for the very long length over which the transition process is seen to take place.

Simultaneous use of blade surface pressure distributions, schlieren visualizations, anemometer fluctuating traces and effective e_{rms} values turn out as a quite effective means for reaching a deeper understanding of transonic blade cascade fluid-dynamics.

ooOoo

REFERENCES

[1] - Pittaluga,F.; Benvenuto,G.: The Adaptive Wall Transonic Wind Tunnels of the University of Genova, Energetics Department, Euromech Colloquium 187, DFVLR-AVA, Göttingen, October 1984.

[2] - Pittaluga,F.; Benvenuto,G.: A Variable Geometry Transonic Facility for Aerodynamic Probe Calibration, in: Proceedings of the 8th Symposium on Measuring Techniques for Transonic and Supersonic Flow in Cascades and Turbomachines, Editors: Troilo,M.; Benvenuto,G.; Pittaluga,F.; Genova, 1986.

[3] - Benvenuto,G.; Pittaluga,F.: Experimental Investigation on the Performances of a Transonic Turbine Blade Cascade for Varying Incidence Angles, XV ICHMT Symposium on Heat and Mass Transfer Measurement Techniques, Dubrovnik, Jugoslavia, September 1983.

[4] - Benvenuto,G.; Pittaluga,F.; Frenna,G.: Flusso transonico in schiere di pale di turbina: confronto tra differenti impianti sperimentali e diverse metodologie di previsione teorica, XXXIX Congresso Nazionale A.T.I., L' Aquila, 1984.

[5] - Italian Register of Industrial Patents - Patents n. 68.019-A/87 and n. 68.020-A/87 - Contact Agency: Italian National Research Council, CNR/PFE, via Nizza 128, Roma.

[6] - Pittaluga,F.; Benvenuto,G.: Contributo all' analisi del comportamento di profili transonici a forte curvatura, Ricerche nel campo delle Turbomacchine motrici, CNR/PFE, Vol. SC-16, Genova, maggio 1988.

[7] - Oldfield,M.L.G.; Kiock,R.; Holmes,A.T.; Graham,C.G.: Boundary Layer Studies on Highly Loaded Cascades Using Heated Thin Films and a Traversing Probe, Trans. ASME J. Engineering for Power, Vol. 103, Jan. 1981.

[8] - Sharma,O.P.; Wells,R.A.; Schinkler,R.H.; Bailey,D.A.: Boundary Layer Development on Turbine Airfoil Suction Surfaces, ASME Paper 81-GT-204 (1981).

[9] - Hilditch,M.A.; Ainsworth,R.W.: Unsteady Heat Transfer Measurements on a Rotating Gas Turbine Blade, ASME Paper 90-GT-175 (1990).

[10] - Moore,M.J.; Sieverding,C.H.: Aerothermodynamics of Low Pressure Steam Turbines and Condensers, Hemisphere Publ. Co., 1987.

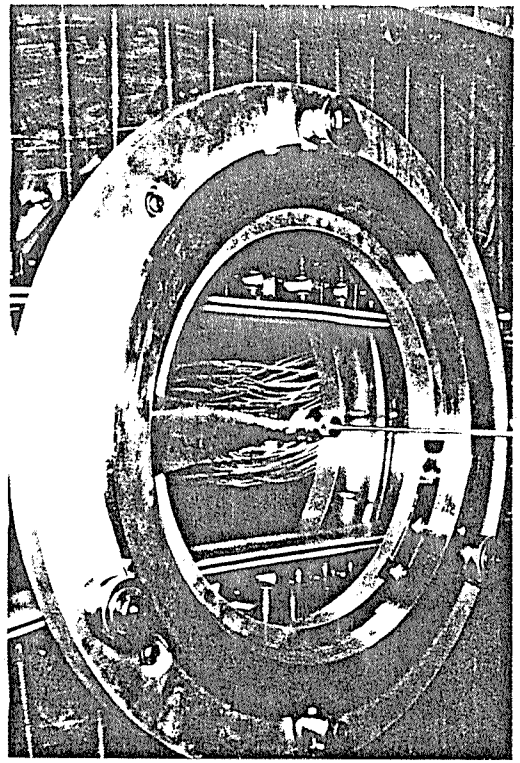

Fig. 1 - Test section of calibration tunnel TRS-1

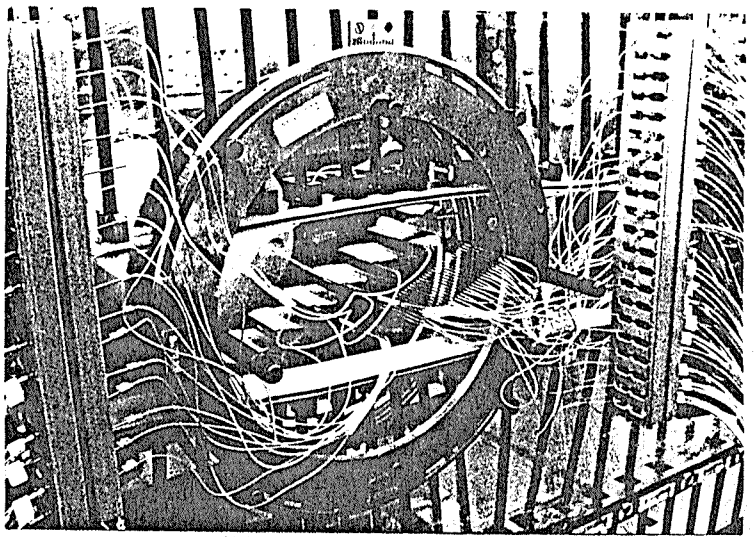

Fig. 2 - Test section of low-deflection blade cascade tunnel TRP-1

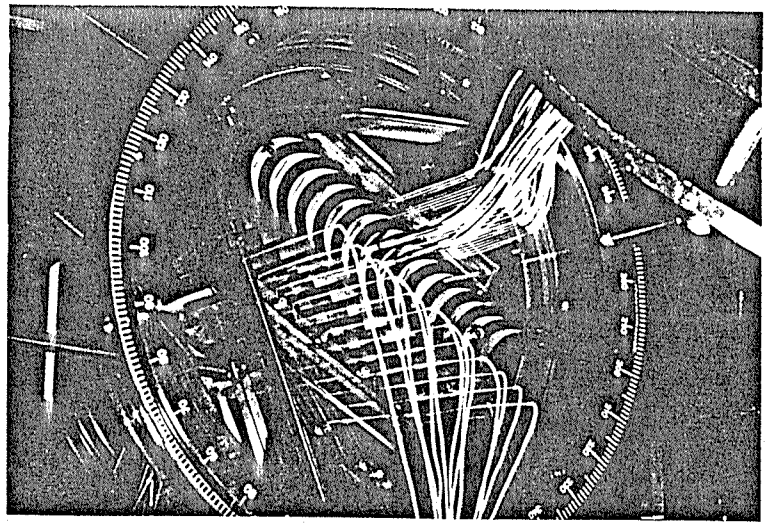

Fig. 3 - Test section of high-deflection blade cascade tunnel TRP-2

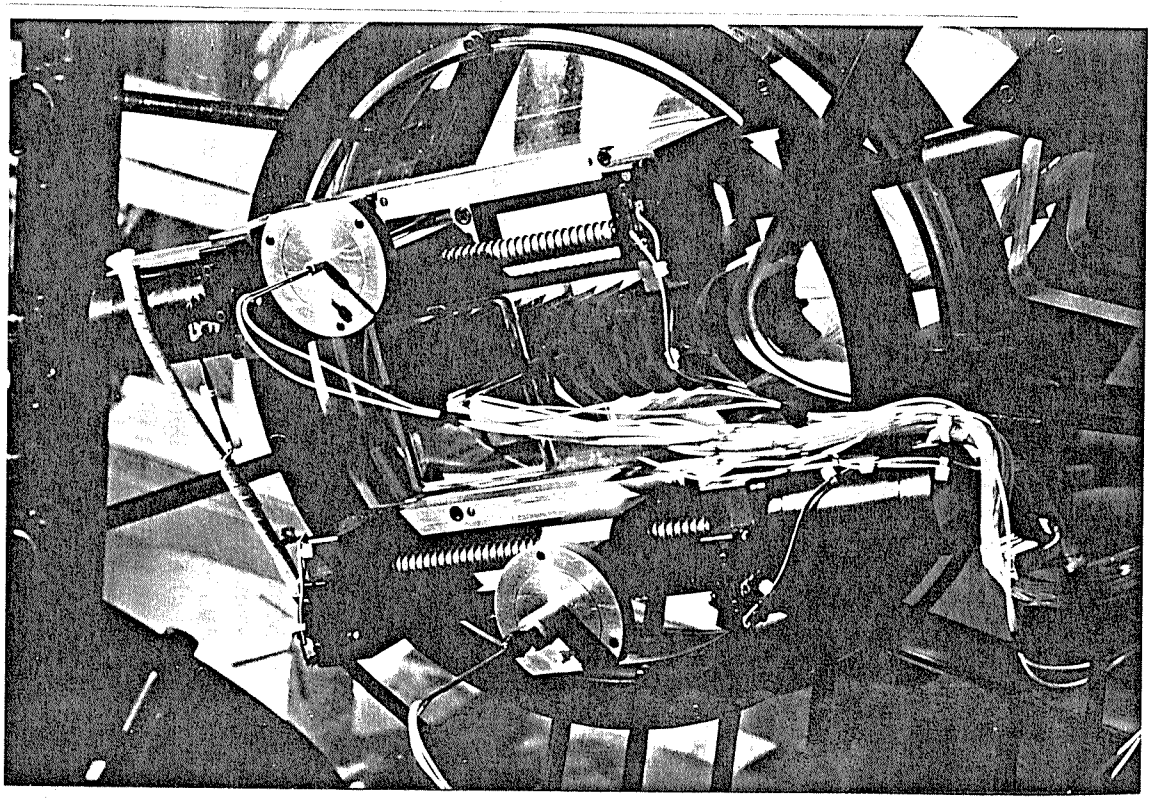

Fig. 4 - Traversing gears of tunnel TRP-2

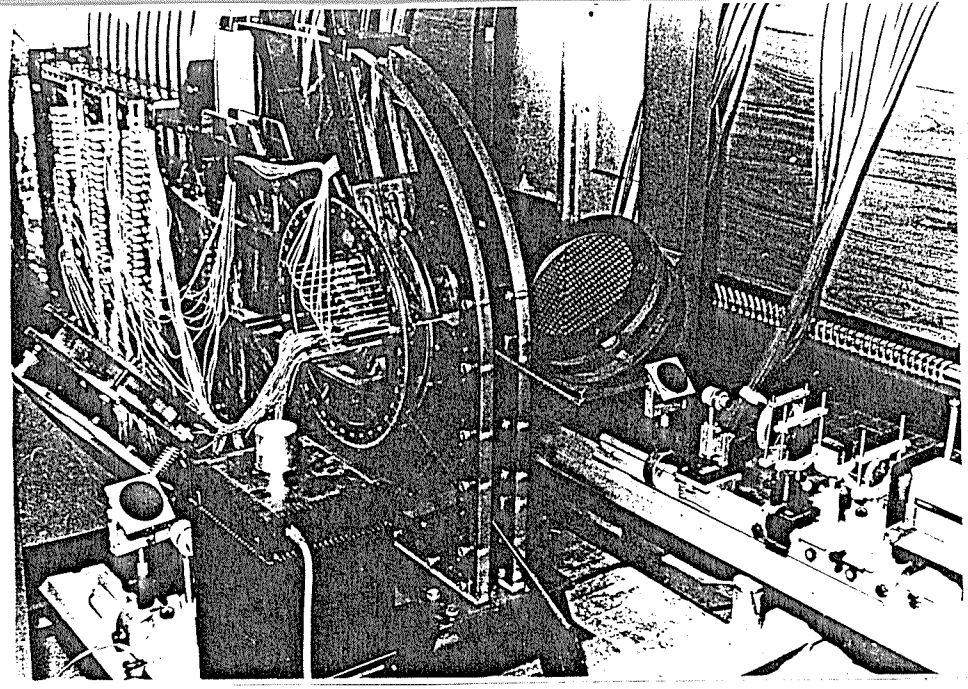

Fig. 5 - Optical instrumentation of tunnel TRP-2

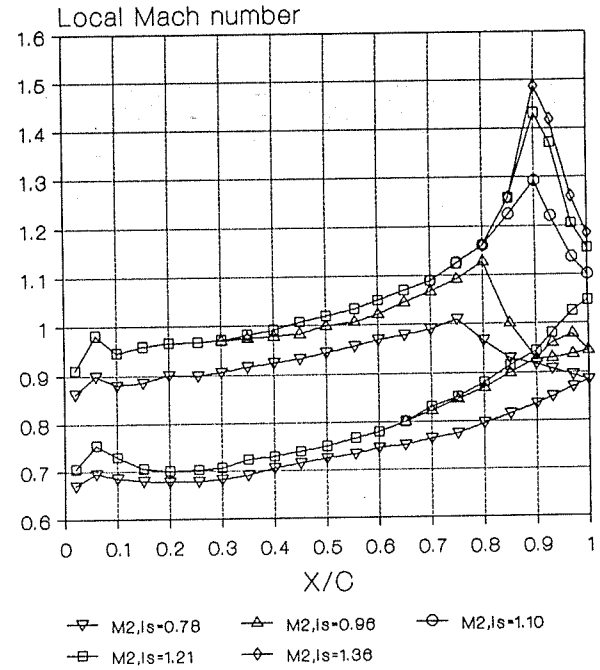

Fig. 6 - Mach number distributions along blade surfaces (experimental)

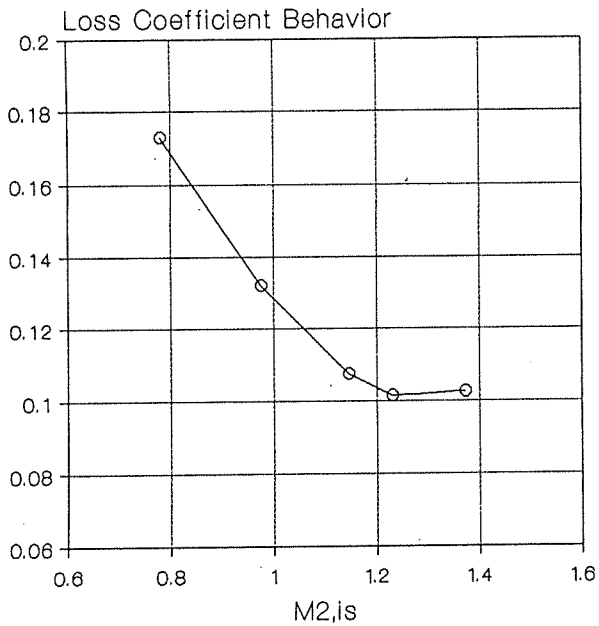

Fig. 7 - Loss coefficient behavior (experimental)

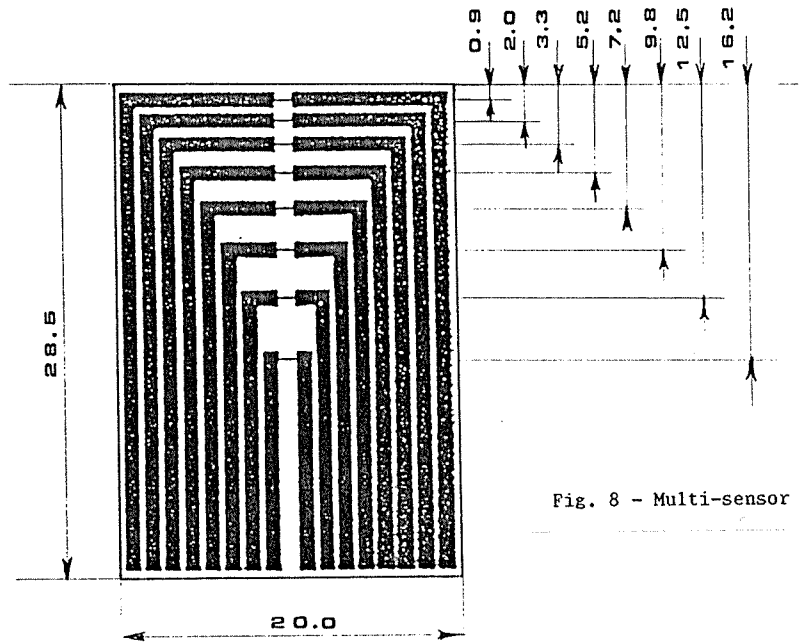

Fig. 8 - Multi-sensor glue-on probe configuration

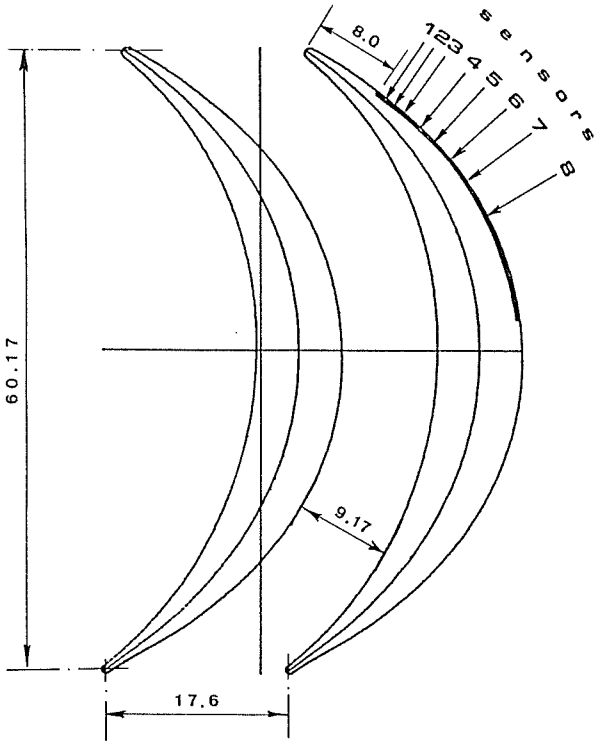

Fig. 9 - Mounting arrangement of the glue-on probe onto the blade

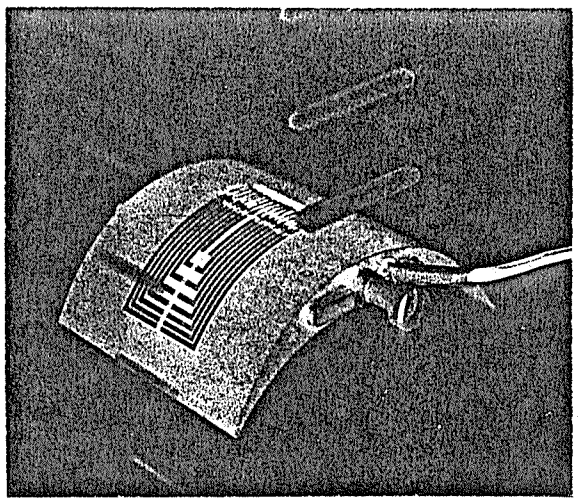

Fig. 10 - An instrumented blade with the flush-on probe

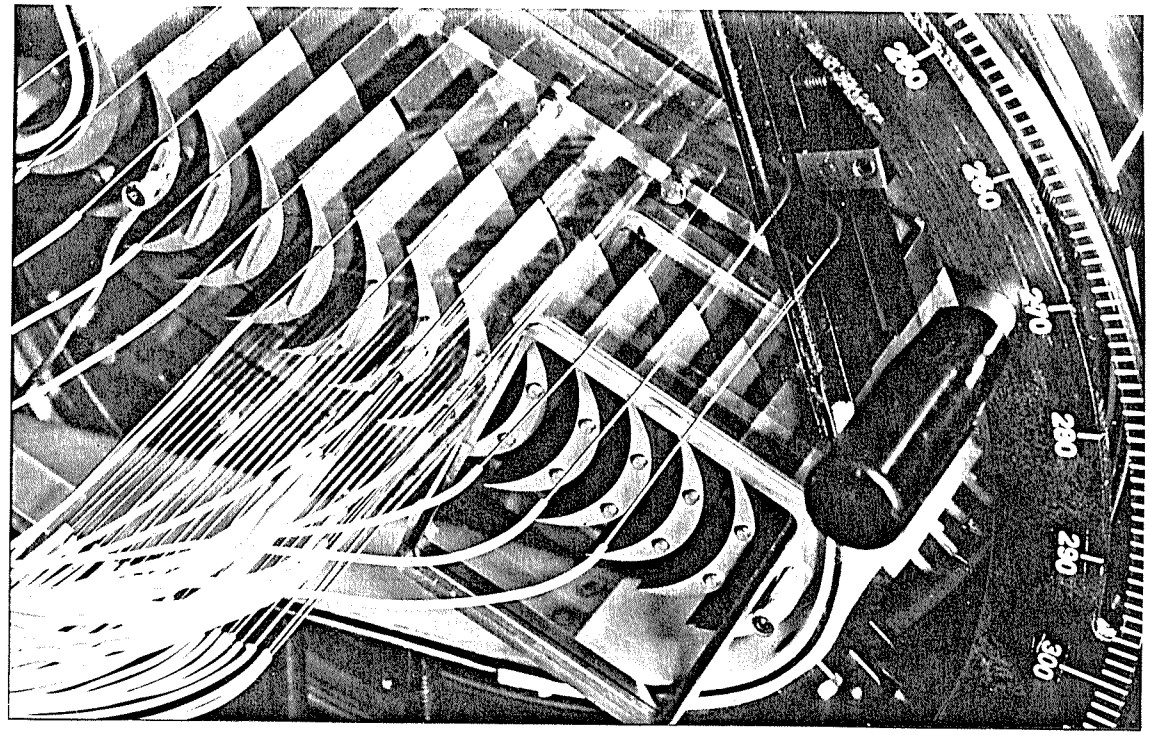

Fig. 11 - The instrumented blade cascade: notice the multi-sensor probe, the optical glass windows and the static pressure instrumented blades.

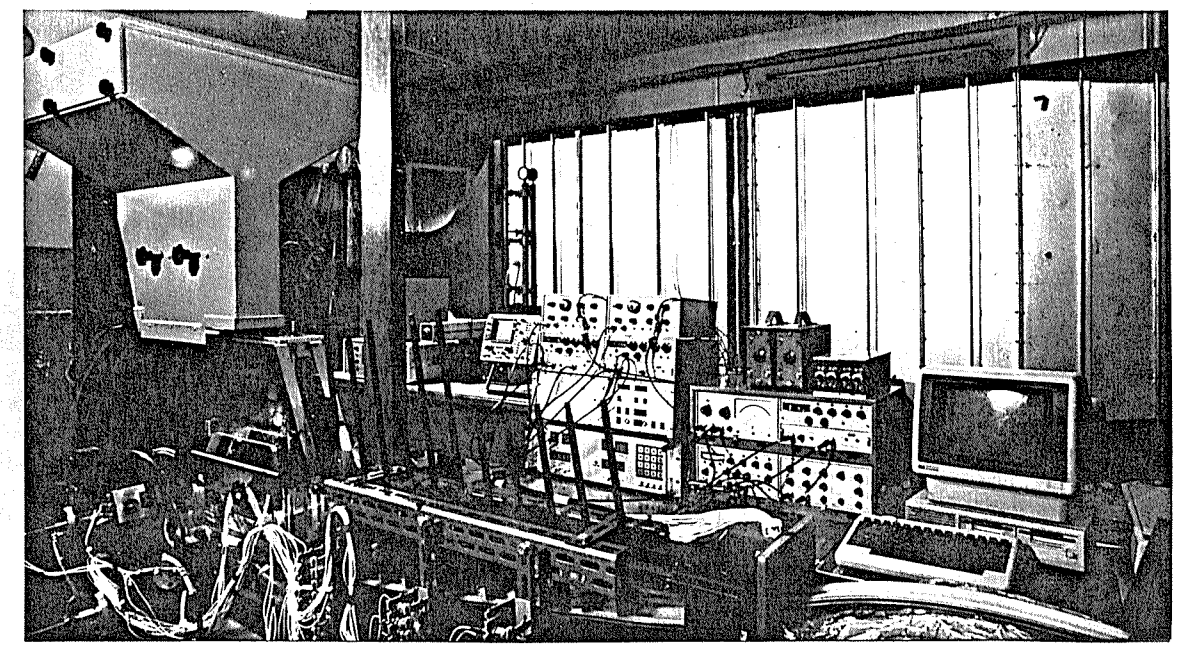

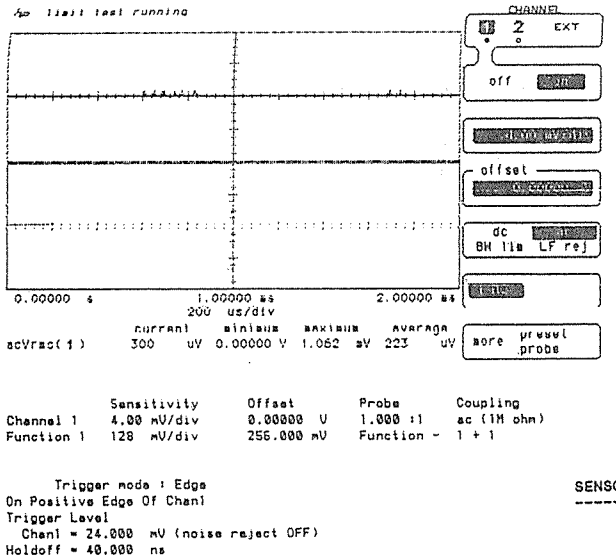

Fig. 13 - Typical no-flow anemometer a.c. output displayed on oscilloscope screen (sensor 1)

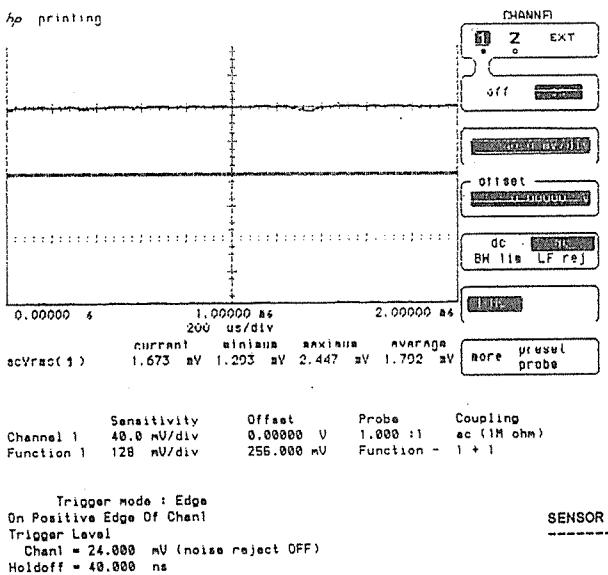

Fig. 14 - Typical laminar-flow output (sensor 1)

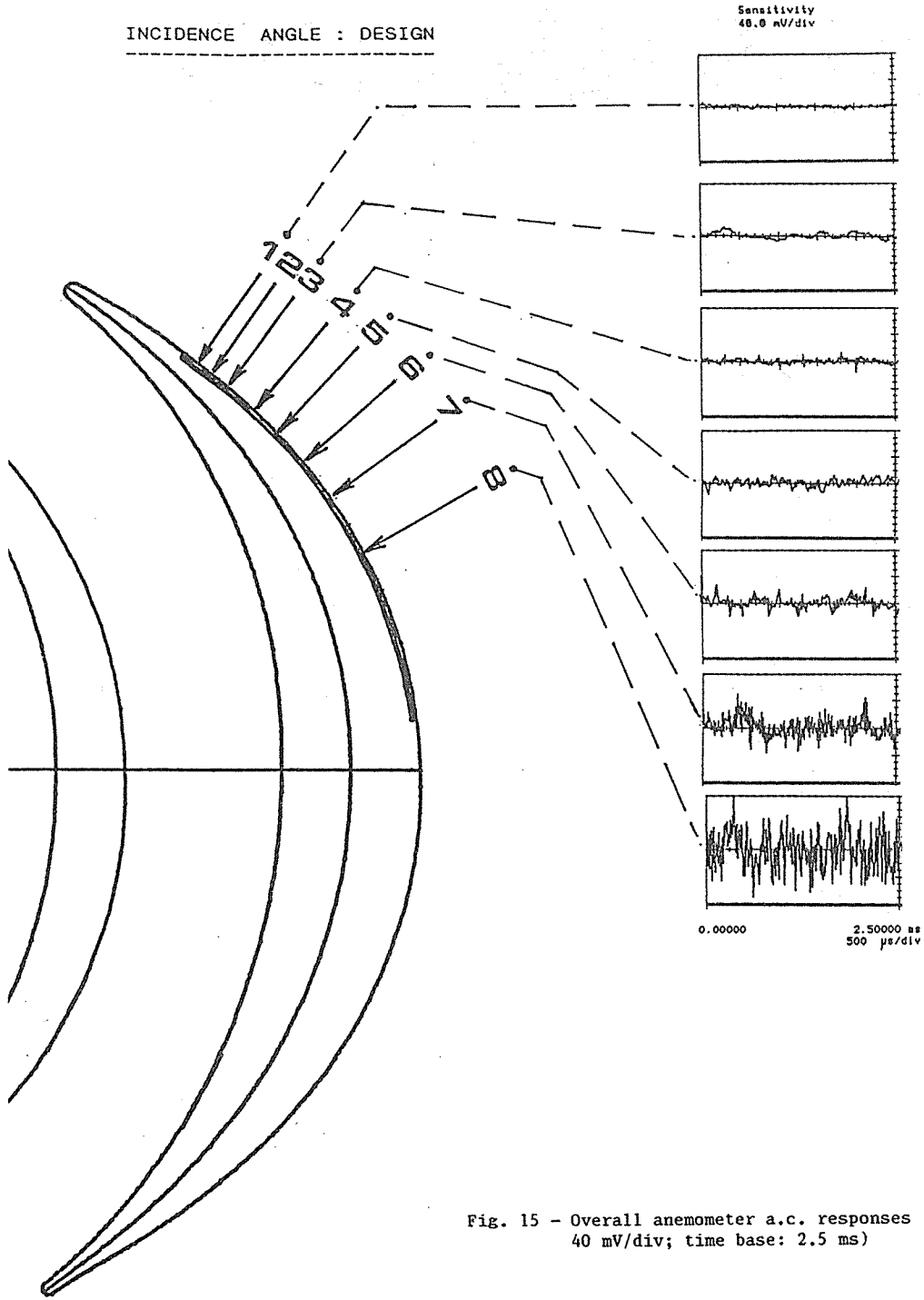

Fig. 15 - Overall anemometer a.c. responses (vertical sensitivity: 40 mV/div; time base: 2.5 ms)

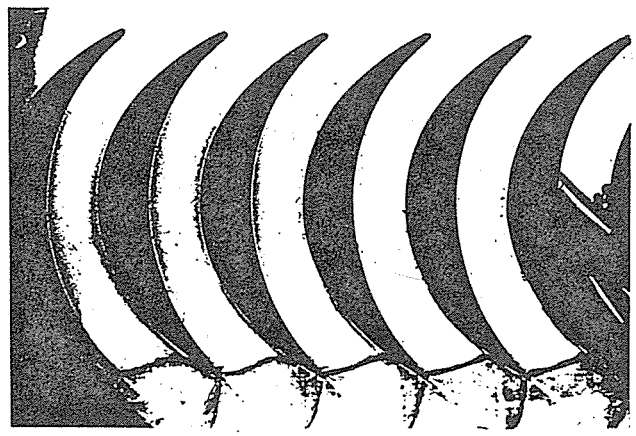

Fig. 16 - Flow visualization

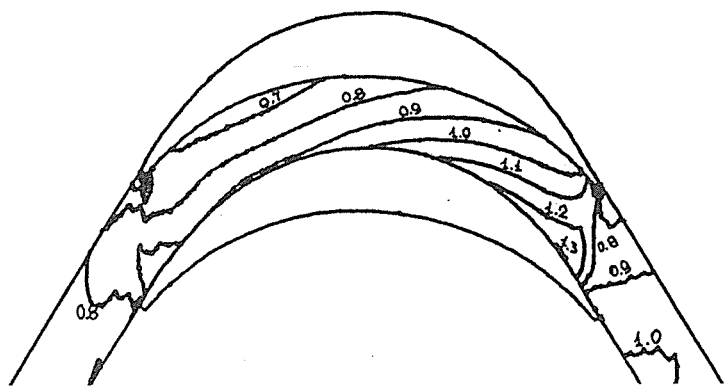

Fig. 17 - Theoretical iso-Mach lines

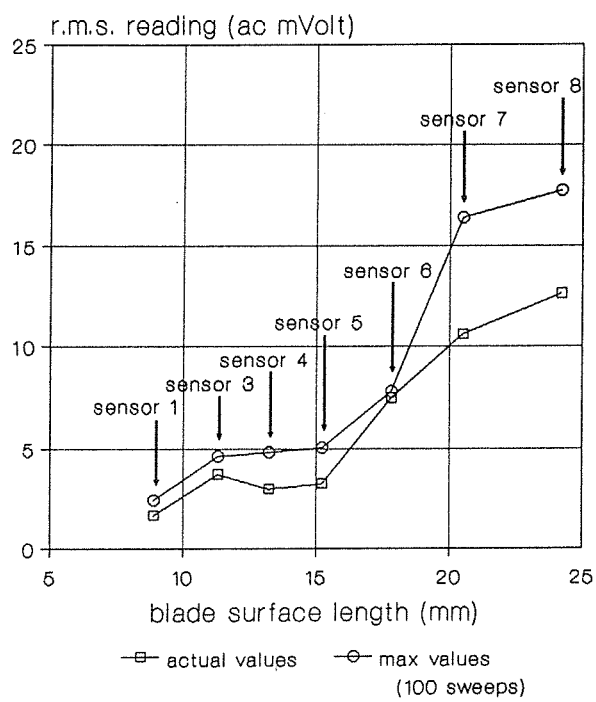

Fig. 18 - Effective (r.m.s.) values of anemometer readings